

# Cyclic Voltammetric Evaluation of Rate Constants for Conformational Transitions Accompanying Electron Transfer. Effect of Varying Structural Constraints in Copper(II/I) Complexes with Dicyclohexanediyl-Substituted Macrocyclic Tetrathiaethers

Nicole M. Villeneuve,<sup>1a</sup> Ronald R. Schroeder,<sup>\*,1a</sup> L. A. Ochrymowycz,<sup>1b</sup> and D. B. Rorabacher<sup>\*,1a</sup>

Departments of Chemistry, Wayne State University, Detroit, Michigan 48202, and University of Wisconsin—Eau Claire, Eau Claire, Wisconsin 54701

Received July 19, 1996<sup>⊗</sup>

Variable-temperature slow- and rapid-scan cyclic voltammetry has been applied in a solvent system of 80% methanol–20% water (w/w) to both the Cu(II) and Cu(I) complexes formed with a series of five ligands in which both of the ethylene bridges in the cyclic tetrathiaether [14]aneS<sub>4</sub> (i.e., 1,4,8,11-tetrathiacyclotetradecane) have been replaced by *trans*- and/or *cis*-cyclohexane. All five substituted complexes exhibit electrochemical behavior which is consistent with the type of dual-pathway electron-transfer mechanism previously observed for the parent Cu<sup>II</sup>([14]aneS<sub>4</sub>) system in which a conformational change is proposed to occur sequentially to the electron-transfer step. The kinetic parameters associated with the formation of the metastable Cu<sup>II</sup>L intermediate cannot be accurately established under the experimental conditions used. However, for the formation of the corresponding metastable Cu<sup>I</sup>L intermediate, both the equilibrium constant and rate constants for the presumed conformational interconversion have been determined with reasonable accuracy. Of the five systems studied, the *meso-trans,trans*- and *dl-trans,trans*-dicyclohexanediyl-substituted ligands show the extremes of behavior in terms of the relative stabilities of the Cu<sup>I</sup>L and Cu<sup>II</sup>L intermediate species. This behavior is shown to be consistent with molecular mechanical calculations for the possible metastable intermediates with these two systems. On the basis of the data obtained in this work, the two electron-transfer pathways are expected to be reasonably competitive for the *dl-trans,trans* derivative but extremely divergent for the *meso-trans,trans* derivative, the relative differences in behavior being attributed to the tendency of the cyclohexane moieties to predispose the four sulfur donor atoms toward the various planar or tetrahedral conformations which can exist for these species. Consideration of the differences to be expected in the internal strains of the various possible conformations of the two oxidation states leads to the hypothesis that these Cu(II/I) systems may actually involve a three-rung ladder mechanism rather than a simple square scheme, although it is doubtful that more than two rungs will ever be experimentally observable.

## Introduction

For redox systems in which the corresponding reductant and oxidant exhibit large differences in geometry, a major portion of the conformational change may occur sequentially, rather than concertedly, with the electron transfer itself; that is, a metastable intermediate may become identifiable. In fact, even in the simplest systems, at least two metastable intermediates may be generated depending upon whether the principal conformational change precedes or succeeds the electron-transfer step. The net result is the generation of at least a dual-pathway square-scheme mechanism of the type illustrated in Figure 1.

In developing a general theoretical treatment for systems of the foregoing type, Hoffman and Ratner<sup>2</sup> noted that the conformational change could, under appropriate conditions, become the rate-limiting process—a condition which they termed *gated electron transfer*. They further proposed that gated behavior might be of exceptional importance in biological systems—such as metalloenzymes—wherein conformational constraints could control the ultimate rate of redox reactions. Brunschwig and Sutin<sup>3</sup> further developed the theoretical description for this type of behavior, noting that, for any specific

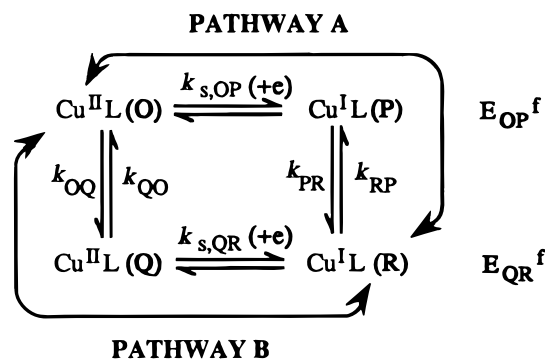


**Figure 1.** Previously proposed dual-pathway square-scheme mechanism for electron transfer in Cu(II/I) systems. The species represented as Cu<sup>II</sup>L(O) and Cu<sup>I</sup>L(R) represent the stable forms of the oxidant and reductant, respectively, while species Cu<sup>II</sup>L(Q) and Cu<sup>I</sup>L(P) are metastable intermediates, presumed to have coordination geometries similar to the stable coordination environments of the other oxidation state.

system, conformational gating should occur *in only one direction* for thermodynamically favorable processes. (The latter authors, therefore, suggested that such behavior be referred to as *directional electron transfer*.)

The concept of conformational control in electron transfer is particularly significant in light of the much earlier *entatic state* (i.e., strained state) hypothesis espoused by Vallee and Williams,<sup>4</sup> who proposed that, particularly in metalloenzymes,

<sup>⊗</sup> Abstract published in *Advance ACS Abstracts*, August 15, 1997.

(1) (a) Wayne State University. (b) University of Wisconsin—Eau Claire.

(2) Hoffman, B. M.; Ratner, M. A. *J. Am. Chem. Soc.* **1987**, *109*, 6237–6243.

(3) Brunschwig, B. S.; Sutin, N. *J. Am. Chem. Soc.* **1989**, *111*, 7454–7465.

constraints placed upon the active site by the surrounding protein matrix might account for the very rapid reactions characteristic of these species. These authors made particular note of the fact that Cu(II) and Cu(I) prefer dramatically different coordination geometries. From this they hypothesized that the imposition of structural constraints could be expected to modulate the observed electron-transfer kinetics of Cu(II/I) systems to a much greater degree than expected for almost any other class of redox-active metal-containing systems.

In previous work, we carefully established the efficacy of the square scheme as a dominant mechanism in the electron transfer of simple inorganic Cu(II/I) systems.<sup>5–10</sup> Under appropriate conditions, we were able to demonstrate the onset of gated behavior. The most thorough characterization of this behavior was conducted on the copper(II/I) complex with the macrocyclic tetrathiaether 1,4,8,11-tetrathiacyclotetradecane ([14]aneS<sub>4</sub>), for which studies included (i) NMR line broadening to establish the self-exchange rate constant under zero driving conditions,<sup>5</sup> (ii) independent evaluation of the self-exchange rate constant under variable driving conditions from the application of the Marcus relationship to cross-reaction kinetics, involving both reducing and oxidizing counterreagents, conducted in both aqueous<sup>5</sup> and acetonitrile<sup>6</sup> solutions, and (iii) extensive cyclic voltammetric studies over a wide range of temperatures to evaluate all of the stepwise rate constants involved in the square-scheme mechanism.<sup>7,8</sup> More limited data were obtained for a few additional systems involving variations in macrocyclic ring size<sup>9</sup> and peripheral substitution on the ligand backbone.<sup>10</sup>

Our most recent studies on two derivatives of [14]aneS<sub>4</sub>, in which one ethylene bridge was replaced by either a *cis*- or *trans*-cyclohexane ring, revealed that significant changes in electron-transfer properties can be induced by relatively simple variations in substitutions on the ligand periphery.<sup>11</sup> To date, however, the available data have been too limited to provide any understanding of the relationship between the introduction of specific conformational constraints and the magnitude of the rate constant associated with the conformational change step and the overall electron-transfer properties.

In the current work, we have undertaken a systematic cyclic voltammetric (CV) study on a closely related series of Cu(II/I) systems in which both ethylene bridges in the [14]aneS<sub>4</sub> ligand are replaced by *cis*- and/or *trans*-cyclohexane rings. The five resulting dicyclohexanediyl-substituted ligands included in this study are illustrated in Figure 2 as ligands L7–L11. Also shown are the parent [14]aneS<sub>4</sub> ligand (L0) and the two corresponding monocyclohexanediyl-substituted analogues (L2 and L3) for which CV data have previously been reported.<sup>7,8,11</sup> The corresponding phenyl derivatives (L1, L4–L6) are included in this figure, although the weakness of their Cu(II) complexes<sup>12</sup>

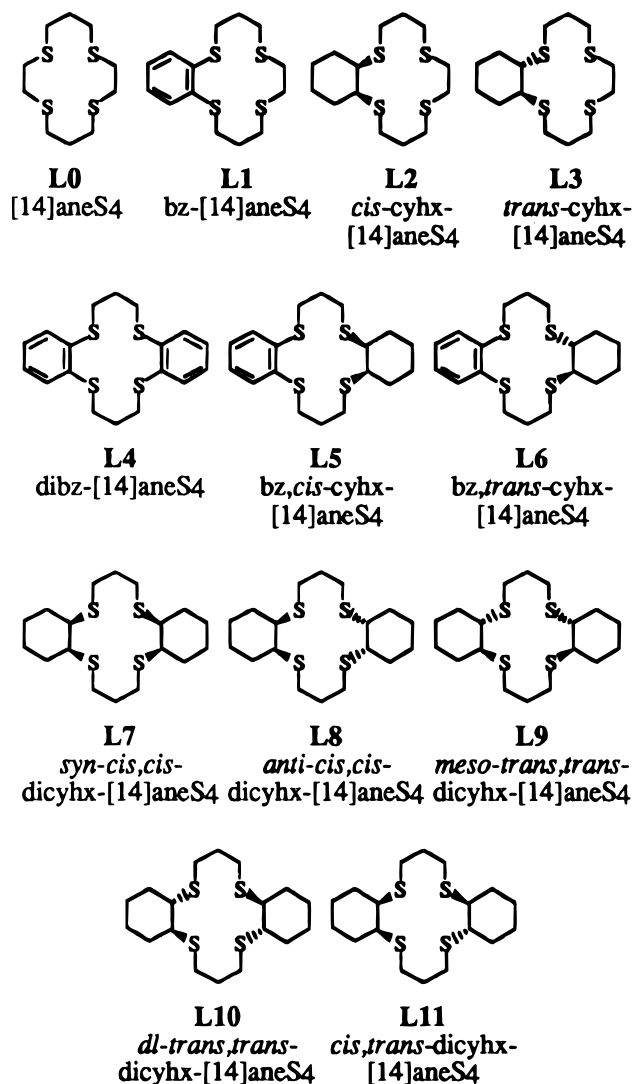


Figure 2. Macrocyclic tetrathiaether ligands discussed in this work.

has made it impossible to obtain viable cyclic voltammetric (CV) data in either aqueous or aqueous–alcoholic media. However, some recent homogeneous electron-transfer studies on the latter systems in acetonitrile<sup>13</sup> permit some relevant qualitative comparisons to be made.

Both slow- and rapid-scan cyclic voltammetric studies have been carried out at three widely separated temperatures on all five dicyclohexanediyl systems in an attempt to characterize each of the stepwise equilibrium and rate constants in the square scheme. Molecular mechanical calculations have also been made for all possible conformers of each Cu<sup>II</sup>L and Cu<sup>I</sup>L complex to determine whether unusual ligand constraints can be identified and correlated to the apparent relative stabilities of the metastable intermediates as well as to the rate constant characteristic of the conformational change which governs the onset of gated electron transfer.

## Experimental Section

**Reagents.** The syntheses of all ligands depicted in Figure 2 along with the thermodynamic properties of their Cu(II) and Cu(I) complexes were previously reported.<sup>12</sup> All electrochemical studies were conducted

- (4) (a) Vallee, B. L.; Williams, R. J. P. *Proc. Natl. Acad. Sci. U.S.A.* **1968**, *59*, 498–505. (b) Williams, R. J. P. *Inorg. Chim. Acta Rev.* **1971**, *5*, 137–155.
- (5) Meagher, N. E.; Juntunen, K. L.; Salhi, C. A.; Ochrymowycz, L. A.; Rorabacher, D. B. *J. Am. Chem. Soc.* **1992**, *114*, 10411–10420.
- (6) Dunn, B. C.; Ochrymowycz, L. A.; Rorabacher, D. B. *Inorg. Chem.* **1995**, *34*, 1954–1956.
- (7) Bernardo, M. M.; Robandt, P. V.; Schroeder, R. R.; Rorabacher, D. B. *J. Am. Chem. Soc.* **1989**, *111*, 1224–1231.
- (8) Robandt, P. V.; Schroeder, R. R.; Rorabacher, D. B. *Inorg. Chem.* **1993**, *32*, 3957–3963.
- (9) Leggett, G. H.; Dunn, B. C.; Vande Linde, A. M. Q.; Ochrymowycz, L. A.; Rorabacher, D. B. *Inorg. Chem.* **1993**, *32*, 5911–5918.
- (10) Meagher, N. E.; Juntunen, K. L.; Heeg, M. J.; Salhi, C. A.; Dunn, B. C.; Ochrymowycz, L. A.; Rorabacher, D. B. *Inorg. Chem.* **1994**, *33*, 670–679.
- (11) Salhi, C. A.; Yu, Q.; Heeg, M. J.; Villeneuve, N. M.; Juntunen, K. L.; Schroeder, R. R.; Ochrymowycz, L. A.; Rorabacher, D. B. *Inorg. Chem.* **1995**, *34*, 6053–6064.

- (12) Aronne, L.; Dunn, B. C.; Vyvyan, J. R.; Souvignier, C. W.; Mayer, M. J.; Howard, T. A.; Salhi, C. A.; Goldie, S. N.; Ochrymowycz, L. A.; Rorabacher, D. B. *Inorg. Chem.* **1995**, *34*, 357–369.
- (13) Dunn, B. C.; Ochrymowycz, L. A.; Rorabacher, D. B. *Inorg. Chem.* **1997**, *36*, 3253–3257.

in 80% methanol–20% water (w/w) to permit the use of subzero temperatures. On the basis of our previous work, the kinetic properties obtained in this solvent mixture appear to be similar to those characteristic of aqueous solutions. The solvent mixtures were prepared from reagent grade methanol (Mallinckrodt, Inc.) and conductivity grade distilled, deionized water.

Copper(II) solutions were prepared by dissolving a weighed sample of pure copper wire (99.9%) in a minimum amount of nitric acid, and the solvent was adjusted to 80% methanol. Ligand solutions were prepared by direct dissolution in 80% methanol and were standardized spectrophotometrically by adding a large excess of Cu(II) followed by the incremental addition of Hg(II) to generate displacement mole ratio plots. All Cu<sup>II</sup>L solutions were prepared to contain a 1:1 mole ratio of Cu(II) and ligand and were allowed to equilibrate overnight before use. The ionic strength was maintained at 0.10 M using sodium nitrate. Cu<sup>I</sup>L solutions were prepared by adding copper shot (Fisher Scientific) to the corresponding Cu<sup>II</sup>L solutions under a nitrogen atmosphere.

**Instrumentation.** Slow-scan cyclic voltammetry was carried out using a BAS 100 electrochemical analyzer (Bioanalytical Systems, Lafayette, IN). A typical three-electrode cell was used with a glassy carbon working electrode (3 mm diameter), a platinum wire auxiliary electrode, and a silver–silver chloride reference electrode ( $E = 0.197$  V vs NHE) from Bioanalytical Systems. The slow-scan measurements were carried out at ambient temperature ( $23 \pm 1$  °C) as well as at  $0 \pm 1$  and  $-23 \pm 1$  °C. For the last two temperatures, the cell was immersed in a shallow Dewar flask containing a NaCl–crushed ice mixture and a dry ice–carbon tetrachloride mixture, respectively.

For rapid-scan cyclic voltammetry, a specially designed instrument was constructed in our laboratory<sup>14</sup> similar to the instrumental setup described by Saveant and co-workers.<sup>15</sup> This instrument was designed to achieve scan rates up to  $10^5$  V s<sup>-1</sup>. The working electrode was a glassy carbon ultramicroelectrode with a 10  $\mu$ m diameter purchased from Cypress Systems, Inc. (Lawrence, KS). Miniature platinum wire auxiliary electrodes and silver–silver chloride reference electrodes were also obtained from Cypress Systems. All rapid-scan measurements were performed within a grounded Faraday cage to minimize 60 Hz interference from the surroundings. For the studies at  $25.0 \pm 0.1$  and  $0.0 \pm 0.1$  °C, the temperature was controlled by circulating a mixture of 50% ethylene glycol–50% water from a constant-temperature bath through a jacket surrounding the electrolytic cell. For the lowest temperature studies ( $-23 \pm 1$  °C), the temperature was controlled with a dry ice–carbon tetrachloride mixture as used for the corresponding slow scans.

The surface of the glassy carbon ultramicroelectrode was cleaned prior to each experiment by sonication followed by polishing with alumina, using the protocol of Rusling and co-workers.<sup>16</sup> The electrode was preconditioned by scanning a blank solution containing only the supporting electrolyte at a constant repetitive rate. The background current was then recorded and subtracted from the subsequent voltammograms. All data were recorded using a Tektronix 2232 oscilloscope. An averaging algorithm, built into the scope software, was used to average the data from several single scans. The averaged digital data were then downloaded to a computer for analysis.

## Results

For each Cu(II/I)–ligand system at each of the three temperatures studied, single-sweep slow-scan cyclic voltammograms (CV's) were obtained at incremental scan rates ranging from 0.01 to greater than  $1.0$  V s<sup>-1</sup>, both for solutions which contained initially only Cu<sup>II</sup>L and for those which contained only Cu<sup>I</sup>L. Rapid-scan CV's were then obtained at varying scan rates ranging from 10 up to  $300$ – $3000$  V s<sup>-1</sup> (and greater) using appropriate instrumentation with the ultramicro working elec-

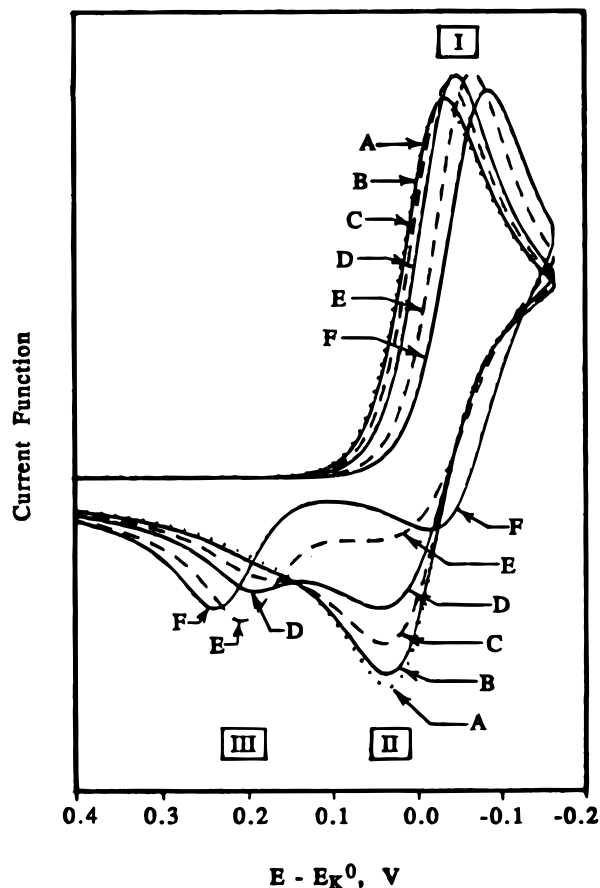
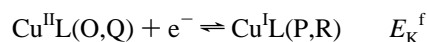


**Figure 3.** General cyclic voltammetric behavior anticipated for Cu<sup>II</sup>L complexes conforming to the dual-pathway square-scheme mechanism depicted in Figure 1 as a function of increasing scan rate. The simulations shown are based on the following typical rate constant values (in s<sup>-1</sup>):  $k_{OQ} = 10^1$ ,  $k_{QO} = 10^5$ ,  $k_{PR} = 10^4$ ,  $k_{RP} = 10^3$ . Scan rates represented are as follows (in V s<sup>-1</sup>): A (···) = 0.010, B (—) = 0.10, C (---) = 1.0, D (- · -) = 10, E (- - -) = 100, F (—) = 1000. All potential values are normalized to  $E_K^0$  (ref 7, Figure 5).

trode. More than 50 CV's were obtained at each temperature for each system, resulting in a total accumulation of nearly 1000 voltammograms for the five systems combined.

For any Cu<sup>II</sup>/I/L system conforming to a dual-pathway square scheme of the type shown in Figure 1, an appropriate increase in the cyclic voltammetric scan rate should alter the appearance of the resulting voltammograms in a characteristic manner.<sup>17</sup> Figure 3 illustrates the general behavior expected for single-scan CV's for any Cu<sup>II</sup>L solution in which the intermediate Cu<sup>I</sup>L(P) is significantly more stable than the intermediate Cu<sup>I</sup>L(Q).<sup>8</sup> The peak designated as peak I represents the reduction of equilibrated Cu<sup>II</sup>L to Cu<sup>I</sup>L at relatively slow scan rates. Peak II represents the corresponding re-oxidation of equilibrated Cu<sup>I</sup>L generated during the reduction half-cycle. These two peaks are used to evaluate the  $E_{1/2}$  value which is presumed to approximate the formal potential value of the equilibrated system, designated as  $E_K^f$ :



Peak III represents the oxidation of the stable Cu<sup>I</sup>L(R) directly to Cu<sup>II</sup>L(Q) under conditions where the scan rate exceeds the rate of conversion of R to the metastable intermediate P. As illustrated by curve F in Figure 3, at very fast scan rates peak

(14) Villeneuve, N. M. Ph.D. Dissertation, Wayne State University, 1995.  
 (15) (a) Saveant, J. M.; Garreau, D.; Hapiiot, P. *J. Electroanal. Chem. Interfacial Electrochem.* **1988**, *243*, 321–335. (b) Saveant, J. M.; Garreau, D.; Hapiiot, P. *J. Electroanal. Chem. Interfacial Electrochem.* **1988**, *248*, 447–450. (c) Saveant, J. M.; Garreau, D.; Hapiiot, P. *J. Electroanal. Chem. Interfacial Electrochem.* **1989**, *272*, 1–16.  
 (16) Kamau, G. N.; Willis, W. S.; Rusling, J. F. *Anal. Chem.* **1985**, *57*, 545–551.

(17) Laviron, E.; Roullier, L. *J. Electroanal. Chem. Interfacial Electrochem.* **1985**, *186*, 1–15.

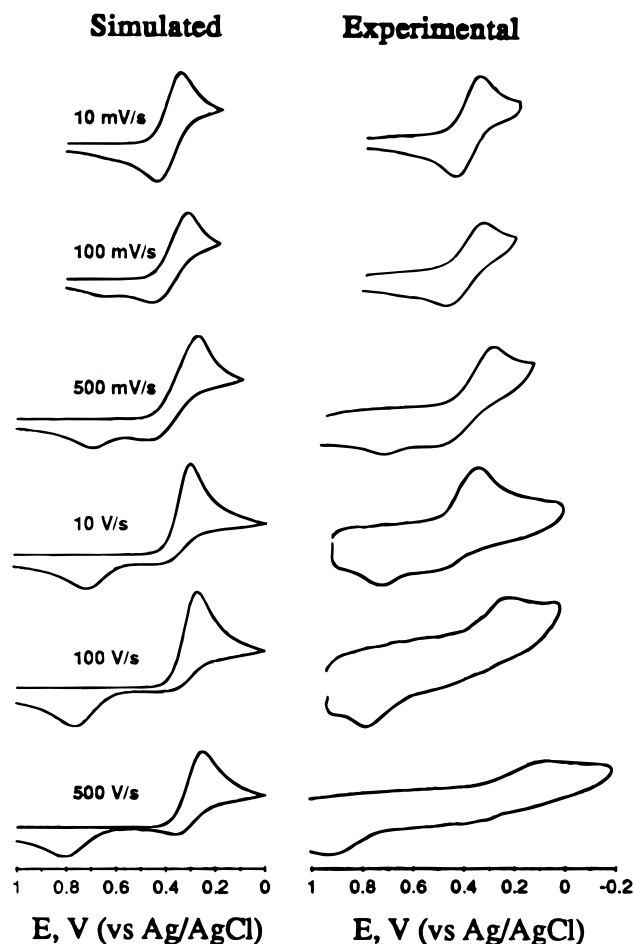


**Figure 4.** Representative cyclic voltammograms for the  $\text{Cu}^{\text{II}}(\text{meso-trans,trans-dicyhx-[14]aneS}_4)$  {i.e.,  $\text{Cu}^{\text{II}}(\text{L9})$ } complex in 80% methanol at 25 °C as a function of scan rate. These peaks demonstrate the development of peak III as the scan rate increases and the beginning of the re-emergence of peak II as the scan rate reaches  $500 \text{ V s}^{-1}$ . The parameters used to generate the simulated voltammograms are listed in Table 1.

III is expected to diminish in size and peak II will re-emerge when the  $\text{Cu}^{\text{I}}(\text{P})$ , generated during the reduction half-cycle, is re-oxidized before it has a chance to convert to  $\text{Cu}^{\text{I}}(\text{R})$ . Since the new peak II represents the direct oxidation of  $\text{Cu}^{\text{I}}(\text{P})$  to  $\text{Cu}^{\text{II}}(\text{O})$ , under conditions where P is no longer equilibrated with R, the position of this new peak II appears at a more negative potential than the original equilibrated peak II and provides a direct estimate of  $E_{\text{OP}}^{\text{f}}$  (Figure 1). The scan rate at which this phenomenon occurs also permits the value of  $k_{\text{PR}}$  (see Figure 1) to be estimated.

A second reduction peak (peak IV), corresponding to the direct reduction of  $\text{Cu}^{\text{II}}(\text{Q})$  to  $\text{Cu}^{\text{I}}(\text{R})$  can become apparent only in solutions initially containing  $\text{Cu}^{\text{I}}(\text{L})$  (or in multiple scans of  $\text{Cu}^{\text{II}}(\text{L})$  solutions) at extremely fast scan rates or very low temperatures.<sup>17</sup> For the most part, this peak was never definitively observed in the current work, indicating that the conversion of the metastable intermediate  $\text{Cu}^{\text{II}}(\text{Q})$  to  $\text{Cu}^{\text{II}}(\text{O})$  is extremely fast in all systems studied in this work.

Figures 4 and 5 contain selected CV's illustrating the experimentally observed features for a single system, *viz.*,  $\text{Cu}^{\text{II}}(\text{meso-trans,trans-cyhx-[14]aneS}_4)$ , as a function of increasing scan rate at 25 °C. The voltammograms are essentially reversible at the slowest scan rate ( $10 \text{ mV s}^{-1}$ ) with clearly defined peaks for the reduction of equilibrated  $\text{Cu}^{\text{II}}(\text{L})$  (peak I) and for the oxidation of equilibrated  $\text{Cu}^{\text{I}}(\text{L})$  (peak II). As the scan rate is increased, the second anodic peak (peak III)

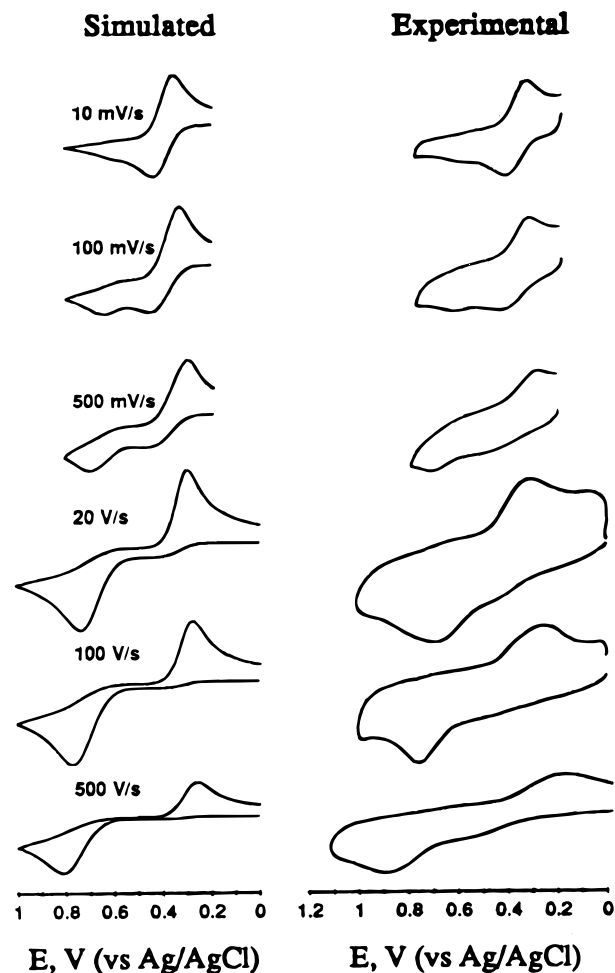


**Figure 5.** Representative single-sweep cyclic voltammograms for the  $\text{Cu}^{\text{II}}(\text{meso-trans,trans-dicyhx-[14]aneS}_4)$  {i.e.,  $\text{Cu}^{\text{II}}(\text{L9})$ } complex in 80% methanol at 25 °C as a function of scan rate. These peaks demonstrate the development of peak III at slower scan rates than required for the corresponding  $\text{Cu}^{\text{II}}(\text{L})$  solutions and the failure of peak II to reappear. The parameters used to generate the simulated voltammograms are listed in Table 1.

immediately develops and eventually becomes dominant. At the fastest scan rate represented in this figure ( $500 \text{ V s}^{-1}$ ), there is a hint that peak II is beginning to re-emerge in the case of the  $\text{Cu}^{\text{II}}(\text{L})$  solution (it will never re-emerge for  $\text{Cu}^{\text{I}}(\text{L})$ )—although problems associated with imperfect background subtraction and *iR* drop are beginning to obscure the CV features. Similar types of behavior were observed for all of the systems investigated in this work, although the scan rates required to bring about changes in peaks II and III varied from system to system, indicative of variances in the values of the rate constants  $k_{\text{PR}}$  and  $k_{\text{RP}}$ .

At the lowest temperature studied ( $-23 \text{ °C}$ ), the voltammograms obtained for  $\text{Cu}^{\text{II}}(\text{L})$  solutions at the more rapid scan rates usually resulted in a more definitive diminution of peak III and the re-emergence of peak II as discussed above. The general absence of an observable peak IV for  $\text{Cu}^{\text{I}}(\text{L})$  solutions in the current work prevented us from making reasonable estimates for the magnitudes of the  $k_{\text{QO}}$  and  $k_{\text{OQ}}$  values. However, the general absence of this peak makes it evident that  $K_{\text{OQ}}$  (the equilibrium constant representing the formation of intermediate Q from O) is generally very small.

On the basis of the changes in the size and positions of peaks I–III as a function of scan rate, the values of  $k_{\text{PR}}$ ,  $k_{\text{RP}}$ , and  $E_{\text{OP}}^{\text{f}}$  were estimated with reasonable accuracy, as previously described,<sup>7,8</sup> at each of the three temperatures studied using the

**Table 1.** Experimental Parameters Obtained from Cyclic Voltammetric Measurements for the Cu<sup>II</sup>/L Redox Couples Involving CyclohexanediyI-Substituted [14]aneS<sub>4</sub> Complexes in 80% Methanol at 25 °C,  $\mu = 0.1$  M (All Parameters Referenced to Figure 1)

parameter	coordinated ligand							
	L0 <sup>a</sup>	L2 <sup>b</sup> <i>cis</i>	L3 <sup>b</sup> <i>trans</i>	L7 <i>syn</i>	L8 <i>anti</i>	L9 <i>meso</i>	L10 <i>dl</i>	L11 <i>cis,trans</i>
$E_K^f$ , V	0.69	0.65	0.70	0.58	0.69	0.61	0.72	0.65
$E_{OP}^f$ , V	0.59	0.55	0.55	0.52	0.56	0.51	0.55	0.54
$E_{QR}^f$ , V	$\leq 1.01$	0.95	0.93	0.90	0.93	0.94	0.89	0.91
$k_{s,OP}$ , cm s <sup>-1</sup>	0.5	0.38	0.30	0.30	0.30	0.38	0.30	0.30
$k_{s,QR}$ , cm s <sup>-1</sup>	0.1–0.3	0.12	0.20	0.20	0.20	0.10	0.30	0.10
$10^{-3}K_{RP}$	20	20	1.9	71	5.3	24	1.1	6.3
$10^{-3}K_{OQ}$	0.04	0.008 <sub>5</sub>	0.2 <sub>0</sub>	0.005 <sub>0</sub>	0.08 <sub>5</sub>	0.001 <sub>9</sub>	1.5	0.007 <sub>0</sub>
$10^{-3}k_{PR}$ , s <sup>-1</sup>	3	22	80	24	160	3.7	130	18
$10^{-3}k_{RP}$ , s <sup>-1</sup>	0.060	0.44	0.15	1.7	0.86	0.090	0.14	0.11
$10^{-3}k_{OQ}$ , s <sup>-1 c</sup>	<i>0.005</i>	<i>0.001<sub>0</sub></i>	<i>0.01<sub>0</sub></i>	<i>0.001<sub>5</sub></i>	<i>0.03<sub>4</sub></i>	<i>0.001<sub>5</sub></i>	<i>0.007<sub>8</sub></i>	<i>0.01<sub>2</sub></i>
$10^{-3}k_{QO}$ , s <sup>-1 c</sup>	<i>1.2 × 10<sup>2</sup></i>	<i>1.1 × 10<sup>2</sup></i>	<i>5.0 × 10<sup>1</sup></i>	<i>3.0 × 10<sup>2</sup></i>	<i>4.0 × 10<sup>2</sup></i>	<i>8.0 × 10<sup>2</sup></i>	<i>5.2</i>	<i>1.7 × 10<sup>2</sup></i>

<sup>a</sup> Reference 8. <sup>b</sup> Reference 11. <sup>c</sup> The  $k_{OQ}$  and  $k_{QO}$  values, listed in italics, represent the values used in performing the computer simulations; they cannot be considered to be accurate, since no distinct peak was observed for the direct reduction of Q → R.

methods established by Nicholson and Shain.<sup>18</sup> A comparison of the  $E_{OP}^f$  and  $E_K^f$  values also permitted us to estimate the magnitude of  $E_{QR}^f$  and, therefore,  $K_{OQ}$ .<sup>8</sup> Values of  $k_{OQ}$  and  $k_{QO}$  were then generated to be consistent with the estimated  $K_{OQ}$  value and the absence of peak IV. For the systems included in this study, the latter values tend to be very approximate since the use of larger values of  $k_{OQ}$  and  $k_{QO}$  did not tend to have a significant effect upon the agreement between the simulated and experimental curves. Therefore, no confidence should be placed in the values reported for the latter rate constants.

Once the initial estimates for the individual rate constants and equilibrium constants were generated directly from the voltammograms, as described above, these values were further refined by computer simulation utilizing a commercial version (DigiSim, Bioanalytical Systems, Lafayette, IN) of Rudolph's accelerated algorithm<sup>19</sup> based on Feldberg's finite-difference method.<sup>20</sup> For this purpose, it was assumed that  $\alpha = 0.5$  and that the diffusion coefficient was  $10^{-5}$  cm<sup>2</sup> s<sup>-1</sup>. As represented in Figures 4 and 5, the simulated curves were compared directly with the experimentally obtained voltammograms and the various individual parameters were successively adjusted until the match between the simulated and experimental curves for all scan rates was optimized. (Allowance was made for the distortions in the rapid-scan voltammograms caused by charging current and incomplete background subtraction.) The latter process generally resulted in a relatively small correction to the original estimates obtained from direct application of Nicholson and Shain's theory. In the selection of the optimal parameters which would most closely match the simulations to the experimental voltammograms, the major focus was to duplicate the peak positions and the relative sweep rates at which the peaks emerged. The actual duplication of peak shape was considered to be of less consequence, particularly since the oxidation of the carbon electrode surface could not be simulated by the software. In recognition of the latter limitation, no attempt was made to simulate the effects of  $iR$  drop and charging current. At sweep rates in the range 10–100 V s<sup>-1</sup>, the

**Table 2.** Thermodynamic Parameters for the R ⇌ P Conformational Change for Cu<sup>II</sup>/L Redox Couples in 80% Methanol at 25 °C,  $\mu = 0.1$  M

parameter	coordinated ligand						
	L2 <i>cis</i>	L3 <i>trans</i>	L7 <i>syn</i>	L8 <i>anti</i>	L9 <i>meso</i>	L10 <i>dl</i>	L11 <i>cis,trans</i>
$\Delta H_{RP}^\circ$ , kJ mol <sup>-1</sup>	27	16	5	9	21	15	12
$\Delta S_{RP}^\circ$ , J mol <sup>-1</sup> K <sup>-1</sup>	-130	-110	-38	-73	-101	-106	-82
$\Delta H_{RP}^\ddagger$ , kJ mol <sup>-1</sup>	23	31	38	41	9	31	29
$\Delta H_{PR}^\ddagger$ , kJ mol <sup>-1</sup>	50	47	43	49	30	46	41
$\Delta S_{RP}^\ddagger$ , J mol <sup>-1</sup> K <sup>-1</sup>	-119	-98	-58	-53	-180	-102	-107
$\Delta S_{PR}^\ddagger$ , J mol <sup>-1</sup> K <sup>-1</sup>	6	9	-19	19	-79	4	-25

voltammograms were somewhat distorted due to spherical diffusion effects of the ultramicroelectrode. However, the peaks were still well-defined and the spherical effects had no impact upon our ability to duplicate peak position or peak emergence and disappearance.

The refined parameters for all five systems at 25 °C are listed in Table 1 along with values generated previously for the Cu<sup>II</sup>/([14]aneS<sub>4</sub>) system<sup>8</sup> and the two monocyclohexanediyI derivatives.<sup>11</sup> All  $E_K^f$  values in 80% methanol were measured against ferrocene for which  $E^f = 0.525$  V in this solvent.<sup>21</sup> The four rate constants for conformational change,  $k_{PR}$ ,  $k_{RP}$ ,  $k_{QO}$ , and  $k_{OQ}$ , are defined in Figure 1, while the two corresponding equilibrium constants are defined as  $K_{RP} = [P]/[R] = k_{RP}/k_{PR}$ <sup>22</sup> and  $K_{OQ} = [Q]/[O] = k_{OQ}/k_{QO}$ . The parameters  $k_{s,OP}$  and  $k_{s,RQ}$  represent the heterogeneous electron-transfer rate constants associated with pathways A and B, respectively (Figure 1). The thermodynamic activation parameters extracted from the temperature dependencies for  $k_{PR}$  and  $k_{RP}$  values are given in Table 2. An understanding of the significance of these values will require the development of more specific information regarding the nature of intermediate P—a topic which will be addressed in future work.

## Discussion

**Rate Constants for Conformational Change.** Of the individual rate constants in Table 1 which are associated with the conformational changes for these systems, the most important value is that of  $k_{RP}$  since the magnitude of this parameter has been shown to govern the onset of gated electron transfer. In fact, for four of the systems listed in Table 1, the value of

- (18) (a) Nicholson, R. S.; Shain, I. *Anal. Chem.* **1964**, *36*, 706–723. (b) Nicholson, R. S. *Anal. Chem.* **1965**, *37*, 667–671, 1351–1355. (c) Nicholson, R. S. *Anal. Chem.* **1966**, *38*, 1406.  
 (19) (a) Rudolph, M.; Reddy, D. P.; Feldberg, S. W. *Anal. Chem.* **1994**, *66*, 589A–600A. (b) Rudolph, M. *J. Electroanal. Chem. Interfacial Electrochem.* **1991**, *314*, 13–22. (c) Rudolph, M. *J. Electroanal. Chem. Interfacial Electrochem.* **1992**, *338*, 89–98.  
 (20) (a) Feldberg, S. W. *J. Electroanal. Chem. Interfacial Electrochem.* **1981**, *127*, 1–10. (b) Feldberg, S. W. *J. Electroanal. Chem. Interfacial Electrochem.* **1987**, *222*, 101–106. (c) Feldberg, S. W. In *Electroanalytical Chemistry. A Series of Advances*; Bard, A. J., Ed.; Marcel Dekker: New York, 1969; Vol. 3, pp 199–296.

(21) See footnote *e* of Table 2 in ref 11.

(22) Note that the value of  $K_{RP}$  is used here instead of that of  $K_{PR}$  as in our previous publications.<sup>7,8</sup> The former quantity is preferred, as it correlates directly with  $K_{OQ}$  in indicating the stability of the intermediate species relative to the corresponding ground state species.

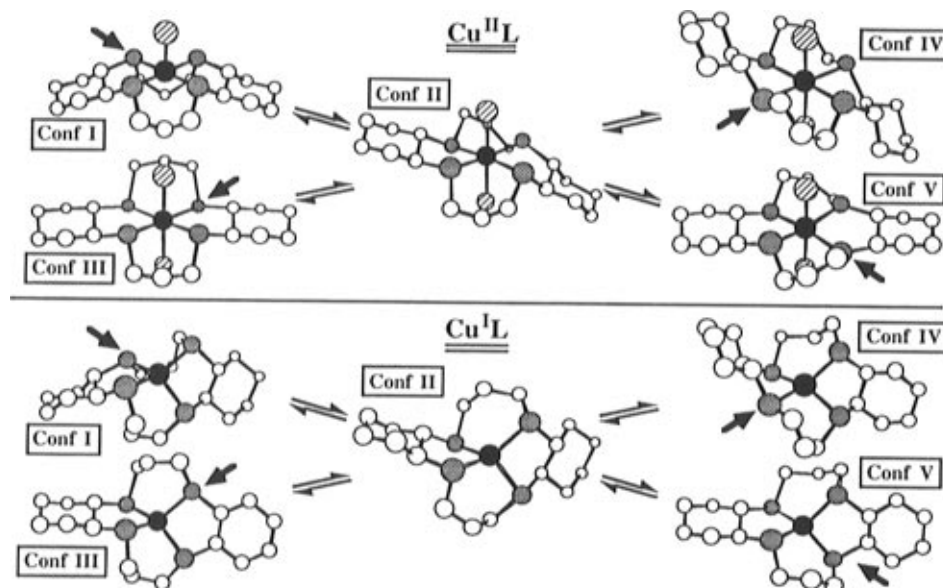


**Figure 6.** Schematic representations of the five conformers possible for  $\text{Cu}^{\text{II}}\text{L}$  and  $\text{Cu}^{\text{I}}\text{L}$  complexes with [14]ane $\text{S}_4$  and its derivatives; *meso-trans,trans*-dicyhx-[14]ane $\text{S}_4$  is utilized in these representations. The solid circles represent the central copper atom, shaded circles represent the sulfur donor atoms, diagonally striped circles are coordinated solvent molecules, and open circles are the carbon atoms. (Hydrogens have been omitted for clarity.) Conformers I, III, IV, and V can convert to Conf II by inverting the sulfur donor atom indicated by the arrow. Conformer I is represented as a five-coordinate species with a single coordinated solvent molecule on the basis of known crystal structures with this conformation (see text).

$k_{\text{RP}}$  has been independently evaluated on the basis of the observation of gated  $\text{Cu}^{\text{I}}\text{L}$  oxidation in homogeneous cross-reactions. For the [14]ane $\text{S}_4$  (L0) system, the value thus obtained<sup>5</sup> was  $50 \text{ s}^{-1}$ , which, as we have previously noted, is in excellent agreement with the cyclic voltammetric value of  $60 \text{ s}^{-1}$ . The  $k_{\text{RP}}$  values determined in the same manner for the *cis*- and *trans*-cyhx-[14]ane $\text{S}_4$  (L2 and L3) systems<sup>11</sup> were 110 and  $32 \text{ s}^{-1}$ , respectively, which compare less favorably with the corresponding cyclic voltammetric values of 440 and  $150 \text{ s}^{-1}$  listed in Table 1. In a very recent study,<sup>13</sup> we have estimated the limiting  $k_{\text{RP}}$  value for the *cis,trans*-dicyhx-[14]ane $\text{S}_4$  (L11) system in acetonitrile at  $\geq 60 \text{ s}^{-1}$ , which is in good agreement with the value of  $110 \text{ s}^{-1}$  determined in the current work (Table 1). (The latter study also yielded a limiting value of  $k_{\text{RP}} \leq 0.3 \text{ s}^{-1}$  for  $\text{Cu}^{\text{I}}(\text{L1})$  (the monophenyl derivative)—considerably smaller than any of the values determined in the current work—which implies that the incorporation of a rigid moiety into the ligand backbone has a significant effect upon the rate constant for conformational change.) Homogeneous cross-reaction studies with the other ligand systems included in the current work are now underway and should provide additional cross-checks on the veracity of the  $k_{\text{RP}}$  data. However, it should be noted that the  $k_{\text{RP}}$  values for the *syn*- and *anti-cis,trans*-dicyhx-substituted ligand systems (L7 and L8) in Table 1 are so large that the onset of gated behavior is unlikely to be observed in cross-reaction studies.

**Comparison of Reaction Pathways.** In our previous electron-transfer studies on  $\text{Cu}^{\text{II}}\text{L}$  systems involving macrocyclic tetrathiaethers, the kinetic evidence indicated that pathway A is the preferred reaction pathway (Figure 1). Thus, in all of the tetrathiaether systems studied to date, the  $\text{Cu}^{\text{I}}\text{L}$  intermediate designated as P must be intrinsically more stable (i.e., “less unstable”) than the  $\text{Cu}^{\text{II}}\text{L}$  intermediate Q.

We previously proposed that the geometry of the  $\text{Cu}^{\text{I}}\text{L}(\text{P})$  intermediate resembles that of the stable  $\text{Cu}^{\text{II}}\text{L}(\text{O})$  complex and that the  $\text{Cu}^{\text{II}}\text{L}(\text{Q})$  intermediate resembles the geometry of the stable  $\text{Cu}^{\text{I}}\text{L}(\text{R})$  species.<sup>7</sup> Wilson, Glass, and co-workers have adopted the same hypothesis in discussing their recent cyclic voltammetric results for  $\text{Cu}^{\text{II}}(\text{[9]aneS}_3)_2$ .<sup>23</sup> On the basis of this

presumption, the greater stability of P relative to Q in our systems has been attributed to the fact that the macrocyclic tetrathiaethers studied to date can more readily adapt to a planar coordination geometry than to a tetrahedral arrangement. The current data provide the first opportunity to examine this hypothesis in terms of the conformational constraints imposed by a series of related substituents on a single-ligand framework.

In Table 1 it is evident from the cyclic voltammetric data that, for all but one system,  $K_{\text{RP}}$  is considerably larger than  $K_{\text{OQ}}$ —that is, intermediate P is, indeed, much more stable than Q. The lone exception is the system involving *dl-trans,trans*-dicyhx-[14]ane $\text{S}_4$  (L10), for which the two equilibrium constants ( $K_{\text{RP}}$  and  $K_{\text{OQ}}$ ) appear to be virtually equal within the limits of experimental error. By contrast, for the closely related *meso-trans,trans*-dicyhx derivative, the apparent stabilities of the P and Q intermediates differ by 4 orders of magnitude. Thus, the two *trans,trans*-dicyhx-substituted systems represent the extremes in behavior in terms of the apparent relative stabilities of the metastable intermediates. These two systems apparently provide a unique opportunity to examine the effects of peripheral substituents upon the preferential conformation of the macrocyclic ligand.

**Copper(II) and Copper(I) Complex Conformations.** The data obtained in this work are of particular interest in terms of the possible conformations of intermediates P and Q. The five possible ligand conformations for six-coordinate  $\text{Cu}^{\text{II}}\text{L}$  and four-coordinate  $\text{Cu}^{\text{I}}\text{L}$  complexes are illustrated in Figure 6. The names applied to these conformers (Conf I, Conf II, etc.) are analogous (but not identical)<sup>24</sup> to those defined previously for octahedral metal complexes with the corresponding cyclic  $\text{N}_4$  ligands.<sup>25–27</sup> Each of the five conformers is distinguished by the chiralities of the coordinated donor atoms—the specific chiralities being most easily visualized in terms of the orientations of the lone electron pairs on the four sulfur donor atoms relative to the macrocyclic ring (“plus” or “minus” being used

(23) (a) Sanaullah; Kano, K.; Glass, R. S.; Wilson, G. S. *J. Am. Chem. Soc.* **1993**, *115*, 592–600. (b) Sanaullah; Hungerbühler, H.; Schöneich, C.; Morton, M.; Vander Velde, D. G.; Wilson, G. S.; Asmus, K.-D.; Glass, R. S. *J. Am. Chem. Soc.* **1997**, *119*, 2134–2145.

to designate "above" or "below" the ring). Thus, for the 14-membered macrocyclic complexes, Conf I may be designated as either *RSRS* or  $++++$  (i.e., all nonbonded electron pairs are in the same orientation relative to the ring), Conf II as *RRRS* or  $+-++$ , Conf III as *RRSS* or  $+-+-$  (the chiralities or lone electron pair orientations being designated in the sequence of the 1,4,8,11-positions), Conf IV as *RSSR* or  $++--$ , and Conf V as *RRRR* or  $+-+-$ . For any interconversion among the various conformers, Conf II must serve as an intermediate species if it is assumed that the donor atom inversions occur one at a time rather than in a concerted manner. For each conformer in Figure 6, the arrow identifies the donor atom which must undergo inversion in converting to Conf II.

Since Cu(I) is known to prefer tetrahedral coordination, Conf V, in which the orientation of the lone pairs alternates around the macrocycle ( $+-+-$ ), is presumed to be the most stable form of Cu<sup>I</sup>L. This premise is supported by the crystal structures previously determined for the perchlorate salts of the Cu(*trans*-cyhx-[14]aneS<sub>4</sub>) complex (i.e., Cu<sup>I</sup>(L3))<sup>11</sup> and by Cu<sup>I</sup>([14]aneNS<sub>3</sub>).<sup>28</sup> In the case of the Cu(II) complexes, either Conf III ( $+-+-$ ) or Conf I ( $++++$ ) is presumed to be most stable by analogy to the cyclic N<sub>4</sub> complexes. The former conformer has been observed in the crystal structure of Cu<sup>II</sup>([14]aneS<sub>4</sub>)<sup>29</sup> and the latter in the crystal structures of Cu<sup>II</sup>(*cis*-cyhx-[14]aneS<sub>4</sub>) and Cu<sup>II</sup>(*trans*-cyhx-[14]aneS<sub>4</sub>).<sup>11</sup> Whereas we have previously presumed that intermediate Cu<sup>I</sup>L(P) approximated a six-coordinate geometry, it is possible that Cu(I) is still four-coordinate but that the distinguishing feature of this intermediate is that it is in the Conf I or Conf III conformation as distinct from Conf V. In a similar fashion, Cu<sup>II</sup>L(Q), which has been presumed to be four-coordinate, may, in fact, remain six-coordinate but represents Conf V. The hypothesis that intermediates P and Q differ from the ground state species in terms of the relative orientations of the donor atoms rather than in terms of the copper coordination number introduces some interesting possibilities for the interpretation of the effect of ligand constraints upon the overall electron-transfer process.

**Molecular Mechanical Estimates of Relative Strain.** In an attempt to establish a more quantitative understanding of the relative magnitudes of the  $K_{OQ}$  and  $K_{RP}$  equilibrium constants, we utilized the SYBYL force field option in the MacSpartan Plus software package (Wavefunction, Inc., Irvine, CA) to examine the relative strain energies in all five conformations of each of the Cu<sup>II</sup>L and Cu<sup>I</sup>L complexes included in Table 1. The energy values obtained after structural minimization are presumed to provide a semiquantitative comparison of the relative strains induced in forcing a specific ligand to adapt to the various conformations. For each complex in each oxidation

state, minimization was approached from several different starting orientations to confirm that the result represents the global, rather than merely a local, minimum for that specific conformer. The results of these calculations are listed in Table 3. In consideration of the limitations of the current calculations, small energy differences are presumed to be of no significance.<sup>30</sup>

It should be stressed that the relative energies for the Cu<sup>II</sup>L species do not correlate to the corresponding values for the Cu<sup>I</sup>L complexes. Therefore, the Cu<sup>II</sup>L and the Cu<sup>I</sup>L energy values should be considered as two independent sets. Furthermore, as a result of the negative inductive effects of the benzene ring, the phenyl derivatives are also expected to involve much different Cu–S force constants so that the relative energies may not be comparable with those of the saturated ligand complexes.

The data in Table 3 are in good qualitative agreement with previous experimental and crystallographic data for cyclic N<sub>4</sub> and S<sub>4</sub> complexes in that the Conf III conformer is generally shown to have the lowest energy for the Cu<sup>II</sup>L complexes closely followed by Conf I; and the Conf V arrangement is least strained for the Cu<sup>I</sup>L species. Among the dicyclohexanediyl derivatives (L7–L11), the energies for each conformer are surprisingly similar—with a few notable exceptions. The values circumscribed by boxes in Table 3 are those which appear to be considerably out of line with the general trends. It is particularly significant that, for the Cu<sup>II</sup>L species, the divergent values involve the two *trans,trans*-dicyhx derivatives, which have been identified in this work as exhibiting the extreme differences in the  $K_{RP}/K_{OQ}$  ratio. Even a simple visual inspection of molecular models leads to the conclusion that the *meso-trans,trans* and the *dl-trans,trans* derivatives twist the sulfur donor atoms in opposite directions; that is, the *meso* ligand readily conforms to a planar (Conf III) conformation, while the *dl* ligand more easily adapts itself to the tetrahedral array of Conf V. This is clearly the most dramatic effect observed for any of the ligands included in this study. As shown in Table 3, the Cu<sup>II</sup>(L10) (*dl*) complex exhibits a relatively large energy for Conf III—confirming the fact that this conformer is unusually strained—and this is the only system for which Conf I is more stable than Conf III for the Cu<sup>II</sup>L species; the corresponding *meso* complex, Cu<sup>II</sup>(L9), shows an unusual degree of strain for both Conf II and Conf V. Since the last conformer has been presumed to most nearly approximate the Cu<sup>II</sup>L(Q) intermediate (see below) and the Conf II species represents a necessary intermediate in converting from Conf I or III to Conf V, these anomalies support the observation that  $K_{OQ}$  is energetically very unfavorable for the *meso-trans,trans* ligand system.

Among energy values for the Cu<sup>I</sup>L complexes with the dicyclohexanediyl-substituted ligands, the most unique appear to be those generated for Conf I in the case of the *meso-trans,trans* and *anti-cis,cis derivatives*—both of which are significantly larger than those for the other ligand systems. However, for reasons outlined below, Conf I may not have a specific bearing upon the electron-transfer mechanism.

**Modifications to the Proposed Mechanistic Pathway.** The foregoing discussion is based on the presumption that the intermediate species, Cu<sup>II</sup>L(Q) and Cu<sup>I</sup>L(P), may represent different ligand conformers relative to the ground state species without necessarily involving differences in coordination number. If the species O and P represent either Conf I or Conf III

- (24) In the earlier nomenclature for quadridentate macrocyclic ligand complexes,<sup>25–27</sup> the conformers were defined as Trans I, Trans II, etc. if the two additional donor atoms (i.e., those not part of the macrocycle) are *trans* to each other or Cis I, Cis II, etc. if they are *cis* (i.e., if the macrocycles are folded). As far as we are aware, no nomenclature has been proposed for the corresponding four- or five-coordinate complexes as encountered in much of this work. For the current nomenclature, Conf I, Conf II, etc. are used to describe the corresponding conformations of any complexes regardless of the coordination number. The same numbering system has otherwise been retained.
- (25) Bosnich, B.; Poon, C. K.; Tobe, M. L. *Inorg. Chem.* **1965**, *4*, 1102–1108.
- (26) Wagner, F.; Mocella, M. T.; D'Aniello, M. J., Jr.; Wang, A. H.-J.; Barefield, E. K. *J. Am. Chem. Soc.* **1974**, *96*, 2625–2627.
- (27) Barefield, E. K.; Bianchi, A.; Billo, E. J.; Conolly, P. J.; Paoletti, P.; Summers, J. S.; Van Derveer, D. G. *Inorg. Chem.* **1986**, *25*, 4197–4202.
- (28) Bernardo, M. M.; Heeg, M. J.; Schroeder, R. R.; Ochrymowycz, L. A. *Inorg. Chem.* **1992**, *31*, 191–198.
- (29) Glick, M. D.; Gavel, D. P.; Diaddario, L. L.; Rorabacher, D. B. *Inorg. Chem.* **1976**, *15*, 1190–1193.

- (30) Minimization of structural error was also carried out using Chem3D Plus (Cambridge Scientific Computing, Inc., Cambridge, MA) including the minimization of all bond length terms, bond angle error terms, planar atom flattening terms, and (where relevant) double-bond-rotation terms: *CSC Chem 3D User's Guide (Version 3.1)*; Cambridge Scientific Computing, Inc.: Cambridge, MA, 1993; p 11-7. The results obtained were in qualitative agreement with the results in Table 3.

**Table 3.** Calculated Molecular Mechanical Approximations to Relative Strain Energies of Alternative Conformers for the Cu(I) and Cu(II) Complexes Formed with CyclohexanediyI and Phenyl Derivatives of [14]aneS<sub>4</sub> (All Values in kJ mol<sup>-1</sup>)<sup>a</sup>

Conformer <sup>c</sup>	Coordinated Ligand											
	L0	L2	L3	L7	L8	L9	L10	L11	L1 <sup>b</sup>	L4 <sup>b</sup>	L5 <sup>b</sup>	L6 <sup>b</sup>
	<i>cis</i>	<i>trans</i>	<i>syn</i>	<i>anti</i>	<i>meso</i>	<i>dl</i>	<i>cis, tr</i>	<i>bz</i>	<i>dibz</i>	<i>bz, tr</i>	<i>bz, cis</i>	
<u>Copper(II) Complexes—Tetragonal Conformers</u>												
Conf I	-25.1	-54.4	-56.1	-82.8	-77.8	-89.1	-83.7	-82.4	-33.1	-41.8	-62.3	-61.9
Conf II <sup>d</sup>	-18.0	-46.4	-32.6	-74.9	-78.2	-42.7	-74.1	-61.5	-21.3	-5.9	-49.0	-52.7
Conf III	-38.5	-66.1	-66.5	-97.5	-97.5	-95.0	-66.9	-94.1	-30.1	-21.3	-58.6	-60.7
Conf IV	+2.9	-22.6	-21.3	-36.4	-48.5	-46.9	-42.7	-46.9	-5.9	-16.7	-29.7	-32.6
Conf V	+22.6	-4.2	-5.0	-33.9	-33.9	+25.5	-32.2	-31.4	+46.9	+74.1	+19.2	+20.9
<u>Copper(I) Complexes—Tetrahedral Conformers</u>												
Conf I	+146	+119	+117	+92	+116	+124	+89	+91	+153	+162	+125	+126
Conf II <sup>d</sup>	+115	+82	+87	+58	+72	+56	+49	+53	+112	+116	+85.8	+86
Conf III <sup>e</sup> (+201)	(+176)	(+176)	(+159)	(+159)	(+184)	(+146)	(+159)	(+213)	(+243)	(+188)	(+188)	
Conf IV <sup>e</sup> +234	+209	+209	(+192)	+186	(+205)	+184	+184	(+238)	(+243)	(+213)	(+218)	
Conf V	+71	+57	+43	+31	+29	+16	+11	+22	+69	+70	+43	+42

<sup>a</sup> All values were calculated using the SYBYL force field option for the MacSpartan Plus software (Wavefunction, Inc.) which does not account for Jahn–Teller distortion (or solvation effects). <sup>b</sup> Although not included in the current work, the phenyl derivatives of [14]aneS<sub>4</sub> are included here (in italics) for purposes of comparison. <sup>c</sup> For description of the various conformers, see text. <sup>d</sup> Two arrangements of Conf II are possible for complexes in which the two substituents differ (i.e., L1, L2, L3, L5, L6, and L11); in all such cases, the energy value for the more stable form is shown. <sup>e</sup> For all Cu<sup>I</sup>L species, energy minimization for Conf III could only be achieved by constraining the positions of four atoms: the 1,4-sulfurs and the attached 5,14-carbons. Similar constraints on three to five atoms were required to achieve minimization for Conf IV for a few Cu<sup>I</sup>L complexes; all “minimal” energies which required such constraints are enclosed in parentheses.

conformers of Cu<sup>II</sup>L and Cu<sup>I</sup>L, respectively, and species Q and R represent Conf V, it is apparent that two sulfur donor atoms must invert during the overall electron-transfer process. On the basis of the assumption that these donor atom inversions occur sequentially, rather than concertedly, both of the processes O ⇌ Q and R ⇌ P must involve the Conf II conformer as an intermediate step, as illustrated in Figure 6.

In theory, any conformer of Cu<sup>II</sup>L could accept an electron to reduce to the corresponding conformer of Cu<sup>I</sup>L. If all five conformers were active in the electron-transfer process, the result would be a “paddle wheel” scheme. (Such a scheme can be envisioned by connecting all five conformer pairs of Cu<sup>II</sup>L and Cu<sup>I</sup>L by vertical electron-transfer steps in Figure 6.) However, not only do the energy values in Table 3 indicate that Conf IV is extremely unstable for Cu<sup>I</sup>L, but this conformation does not serve as a viable intermediate in generating any of the stable species for either oxidation state. Therefore, it can almost certainly be ruled out as a viable intermediate in the electron-transfer mechanism. If we may further conclude that either Conf I or Conf III is likely to be favored for any specific Cu<sup>II</sup>L complex, while Conf V (R) is the favored structure for Cu<sup>I</sup>L and that each sulfur inversion occurs sequentially, the minimal mechanism can be described as a three-rung ladder scheme as illustrated in Figure 7. (In this figure, Conf I is not represented since it is apparent that Conf III will generally predominate as the stable form of Cu<sup>II</sup>L. The inclusion of both Conf III and Conf I results in a three-rung stepladder scheme with a bifurcated top step.)

In Figure 7, the Q intermediate from Figure 1 is replaced by two possible Cu<sup>II</sup>L intermediates designated as W (Conf II) and X (Conf V) while the P intermediate is replaced by Y (Conf III) and Z (Conf II). Three reaction pathways are then feasible for the reduction of O to R: (i) O ⇌ Y ⇌ Z ⇌ R (top rung),

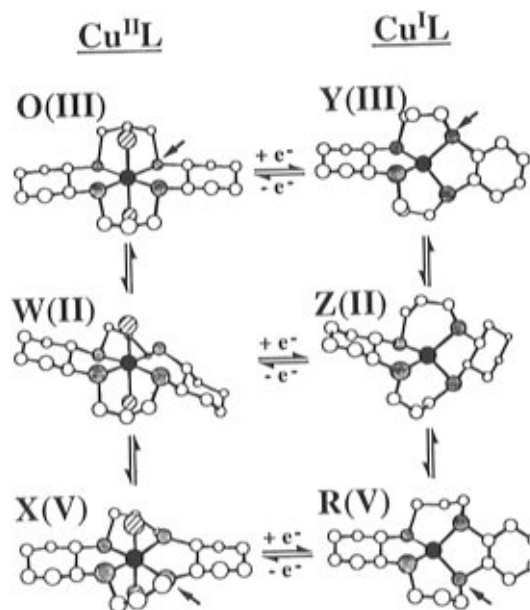


**Figure 7.** Proposed three-rung ladder scheme for Cu(II/I) electron transfer involving [14]aneS<sub>4</sub>-type complexes. Conformers are identified in parentheses. Vertical reactions represent conformational changes, while horizontal reactions involve electron transfer. The arrows in species O, X, Y, and R indicate the sulfur atom which must undergo inversion in converting to species W and Z, respectively. The current analysis suggests that species Y is not important for the current systems, while X and Z correspond to Q and P, respectively, in Figure 6 (see text). Species O and W are presumed to be in rapid equilibrium at all times and are, therefore, indistinguishable in the electron-transfer kinetics.

(ii) O ⇌ W ⇌ Z ⇌ R (middle rung), and (iii) O ⇌ W ⇌ X ⇌ R (bottom rung).



Ladder schemes of the type represented in Figure 7 are relatively uncommon;<sup>31</sup> but they have been proposed for some redox-active metal complexes in which multiple conformers are known to be possible. Mevs and Geiger<sup>32</sup> have studied the voltammetric behavior of a rhodium-carbonyl cluster, for which they suggested that three conformers might be active. Bond and co-workers have provided a detailed analysis of the  $\text{Co}^{\text{III/II}}(\text{dien})_2$  system,<sup>33</sup> for which they proposed the existence of a three-rung ladder scheme, similar to that in Figure 7.

On the basis of the presumption that the three-rung ladder scheme in Figure 7 is viable for our systems, it is highly unlikely that all three pathways will ever be uniquely observed. If the intermediate W is at all times in rapid equilibrium with either O or X, and if Z is similarly in equilibrium with either Y or R, only a square scheme will be evident from the experimental data. As a result, when two pathways are observed, as in the current study, it is impossible to specify whether these correspond to pathways i and ii, to pathways i and iii, or to pathways ii and iii as designated above. However, some relevant hypotheses regarding the possible alternatives can be made.

In consideration of the fact that, for all  $\text{Cu}^{\text{II/L}}$  species included in this work, the Conf V conformation is *much* less stable than Conf II, pathway ii (middle rung) is presumed to be more favorable than pathway iii (bottom rung). From the calculations in Table 3, it would also appear that, among  $\text{Cu}^{\text{II/L}}$  species, Conf II is much more stable than Conf I and Conf III. On the basis of these considerations, we conclude that the middle rung pathway ii is likely to be the most favored pathway represented by the experimental data. The fact that  $K_{\text{RP}}$  is, in all cases, smaller than  $K_{\text{OQ}}$  implies that the other observable pathway must be represented by the bottom rung (iii). Thus, we propose that pathway A correlates to  $\text{O} \rightleftharpoons \text{W} \rightleftharpoons \text{Z} \rightleftharpoons \text{R}$  (middle rung) and pathway B is represented by  $\text{O} \rightleftharpoons \text{W} \rightleftharpoons \text{X} \rightleftharpoons \text{R}$  (bottom rung).

(31) Evans, D. H. *Chem. Rev.* **1990**, *90*, 739–751.

(32) Mevs, J. M.; Geiger, W. E. *J. Am. Chem. Soc.* **1989**, *111*, 1922–1923.

(33) Bond, A. M.; Hambley, T. W.; Snow, M. R. *Inorg. Chem.* **1985**, *24*, 1920–1928 (dien = diethylenetriamine, i.e., 1,4,7-triazaheptane).

Intermediate Q would then correspond to X and intermediate P would be identified as Z. This hypothesis implies that intermediate W is, in all cases, in rapid equilibrium with O and is not distinguishable as a separate species; it is also implied that species Y is never a competitive intermediate.

The foregoing conclusions are in agreement with our previous arguments that pathway B cannot be the lowest energy pathway for the majority of these macrocyclic  $\text{S}_4$  ligand systems since the conformational change represented by  $k_{\text{RP}}$  has been observed to become the rate-determining process during the oxidation of  $\text{Cu}^{\text{II/L}}$  in homogeneous cross-reactions involving complexes formed with the ligands L0,<sup>5</sup> L2 and L3,<sup>11</sup> and L1, L5, and L6.<sup>13</sup>

**Implications.** The electrochemical data generated in the current work bear out the prediction that peripheral substitutions can cause changes in the preferred orientation of the donor atoms in a macrocyclic ligand, which, in turn, can cause significant differences in the electron-transfer properties of  $\text{Cu}(\text{II/I})$  complex systems where large conformational changes are involved. Of the systems included in the current work, the  $\text{Cu}^{\text{II/L}}$  systems involving the *meso-trans,trans*-dicyhx and *dl-trans,trans*-dicyhx derivatives of [14]ane $\text{S}_4$  exhibit uniquely different  $K_{\text{RP}}/K_{\text{OQ}}$  ratios suggesting that the “two” electron-transfer pathways in the observable square scheme should be competitive for the *dl* derivative such that no gated electron transfer should be apparent in homogeneous oxidation reactions of  $\text{Cu}^{\text{II/L}}$ . By contrast, the onset of gated electron transfer should be readily observed for the oxidation of the *meso-trans,trans* complex,  $\text{Cu}^{\text{II/L}}$ (L9), and should result in a wide gated region. These last predictions are currently being investigated in an extensive series of studies using a wide variety of homogeneous cross-reactions with the *meso* and *dl* systems. The other three dicyclohexanediy derivatives will also be included in this work for purposes of comparison.

**Acknowledgment.** This work was supported by the National Science Foundation under Grant CHE-9218391.

IC960866Z